Hard-core bosons in one-dimensional interacting topological bands

Huaiming Guo
Department of Physics, Beihang University, Beijing 100191, China
(Received 31 July 2012; published 30 November 2012)

We study the hard-core bosons in one-dimensional (1D) interacting topological bands at different filling factors using exact diagonalization. At the filling factor $\nu = 1$ and in the presence of the on-site Hubbard interaction, we find no sign of the existence of the bosonic topological phase, which is in contrast to the fermionic case. Instead by studying the momentum distribution and the condensate fraction we find a superfluid to Mott-insulator transition driven by the Hubbard interaction. At the filling factor $\nu = 1/3$ and in the presence of longer-ranged interactions, we identify the bosonic fractional topological phase whose ground states are characterized by a threefold degeneracy and a quantized total Berry phase, which is very similar to the fermionic case. Finally we discuss the reason for the different behaviors of hard-core bosons at different filling factors by mapping them to spinless fermions. Our results can be realized in cold-atom experiments.

DOI: 10.1103/PhysRevA.86.055604 PACS number(s): 03.75.Hh, 03.65.Vf, 71.10.Fd

Introduction. Recently topological insulators (TIs) have been the subject of intense theoretical and experimental studies [1,2]. Till now many materials have been found to be TIs. The properties of noninteracting TIs have been well understood and some of their important properties have been verified by experiments [3–5]. Meanwhile the effects of interactions in TIs have begun to be explored numerically and analytically [6–12]. At the mean-field level, the interaction can be decoupled to generate spin-orbit coupling and a topological Mott insulator can be realized [6]. Numerical simulations using different methods have obtained consistent results [7–11]. The interacting topological invariant has been developed using Green's function and a simplified formula has been proposed in terms of the Green's function at zero frequency or in the presence of inversion symmetry [13–15]. The effects of interactions on the topological classification of free fermion systems have also been studied [16,17].

By analogy with TIs, models that exhibit nearly flatbands with nontrivial topology are constructed in different systems, in which fractional Chern insulators (FCIs) may be realized in the absence of external magnetic fields [18–29]. The phase is characterized by a multifold degenerate ground state with a quantized total Chern number. By combining the two copies of FCIs formed by spin-up and spin-down electrons, fractional TIs with time-reversal symmetry can be constructed, which will be another new quantum state of matter.

In real materials, properties are usually exhibited by electrons that are fermions, so most of the above studies are for fermions. It is also interesting to ask whether there exist similar topological phases in bosonic systems. Studies in two dimensions have been carried out and the properties of hard-core bosons in topological bands have been investigated [7,29]. In this paper, based on our study of the one-dimesional (1D) interacting fermionic model [30,31], we study the behavior of hard-core bosons in 1D topological bands using exact diagonalization.

We study the cases of the filling factors $\nu = 1$ and $\nu = 1/3$. For the case of $\nu = 1$, we consider the on-site Hubbard interaction. By calculating the energies of the lowest states, the Berry phase, and the fidelity metric of the ground states, we find no sign of the existence of the bosonic topological phase. We further calculate the momentum distribution and the condensate fraction and find a superfluid (SF) to Mott-insulator transition driven by the Hubbard interaction. For the case of $\nu = 1/3$, we consider nearest-neighboring (NN) and next-nearest-neighboring (NNN) interactions. We identify the bosonic fractional topological phase (FTP) whose ground states are characterized by a threefold degeneracy and a quantized total Berry phase. The obtained phase diagram is very similar to that of the corresponding fermionic system except for the different critical values. Finally we discuss the reason for the different behaviors of the hard-core bosons at different filling factors.

The model. Our starting point is the 1D interacting tight-binding model filled with hard-core bosons [30],

$$H = \sum_i (M + 2B)\Psi_i^\dagger \sigma_z \Psi_i - \sum_{i,\hat{x}} B\Psi_i^\dagger \sigma_z \Psi_{i+\hat{x}} - \sum_{i,\hat{x}} \mathrm{sgn}(\hat{x}) i A \Psi_i^\dagger \sigma_x \Psi_{i+\hat{x}} + U \sum_i n_i^c n_i^d, \quad (1)$$

where σ_x and σ_z are Pauli matrices; $\Psi_i = (c_i, d_i)^T$, with c_i (d_i) hard-core boson annihilating operator at the site $\mathbf{r}_i$; and n_i^c (n_i^d) is the number operator of orbit c (d). In the fermionic version of the noninteracting model ($U = 0$), depending on the values of the parameters A, B, and M, the system can be a trivial insulator or a nontrivial insulator at half-filling. Though like spinless fermions the occupying number of hard-core bosons is 0 or 1 per orbit on each site, the hard-core bosons obey commutation relation $[c_i, c_j^\dagger]([d_i, d_j^\dagger]) = 0$ at sites $i \neq j$ but anticommutation $\{c_i, c_i^\dagger\}(\{d_i, d_i^\dagger\}) = 1$ on only site i, which makes the hard-core bosons exhibit different properties from the fermions. In the following calculations, we focus on the parameters' region where the Hamiltonian Eq. (1) at $U = 0$ has a nontrivial fermionic topological phase and we study the properties of hard-core bosons in the interacting topological bands at different fillings.

The filling factor $\nu = 1$. We first study the case of the filling factor $\nu = 1$ (we denote the number of particles as N_p and the filling factor is $\nu = N_p/L$). To characterize the possible phases and phase transitions in the system, we calculate the energies E_n of the two lowest states, the Berry phase γ, and the fidelity metric g of the ground state. The Berry phase is defined as $\gamma = \oint i \langle \psi_\theta | \frac{d}{d\theta} | \psi_\theta \rangle$ with θ being the twisted boundary phase

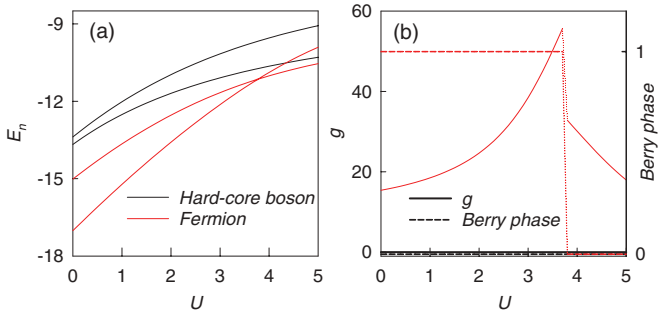

FIG. 1. (Color online) (a) The energies of the ground states and the first-excited states vs U. (b) The Berry phase and the fidelity metric vs U. The results in bosonic (black, top two lines) and fermionic (red, bottom two lines) systems are compared. The parameters are $A = B = 1$ and $M = -1$, and the system size is $L = 8$.

and its value γ mod 2π gets a nonzero value π for the topological phase and a zero value for the trivial phase [32–34]. The fidility metric g is defined as $g(V,\delta V) = \frac{2}{N}\frac{1-F(V,\delta V)}{(\delta V)^2}$, with the fidelity $F(V,\delta V) = |\langle\Psi_0(V)|\Psi_0(V+\delta V)$ being the overlap of the two ground-state wave functions at V and $V + \delta V$ [7]. When the topological band is filled with hard-core bosons, as U is increased, it is shown in Fig. 1 that the ground state remains gapped and $\gamma = 0$ and $g = 0$ all the way, indicating that no obvious phase transition happens. This is in contrast to the fermionic case, where the Hubbard interaction U drives a topological phase transition [30].

So the topological property doesn't persist when hard-core bosons replace the fermions. To identify the bosonic phase, we study the momentum distribution, which is defined by the formula [35]

$$n_L(k) = \frac{1}{L}\sum_{i,j=0}^{L-1}\langle c_i^\dagger c_j + d_i^\dagger d_j\rangle e^{ik(i-j)},$$

with the momentum $k = (2\pi/L)l (l = 0,1,\ldots,L-1)$ and the average $\langle\cdots\rangle$ over the ground-state wave function. As has been known for free hopping bosons, the ground state is a SF, which is characterized by the peak at the zero-momentum state and its height strongly depending on L. In our case of $U = 0$ (see Fig. 2), the momentum distribution shows peaks at $k = \pi/2$ and $3\pi/2$ and their height increases with the size L. Thus the results show that the system is in a trivial SF

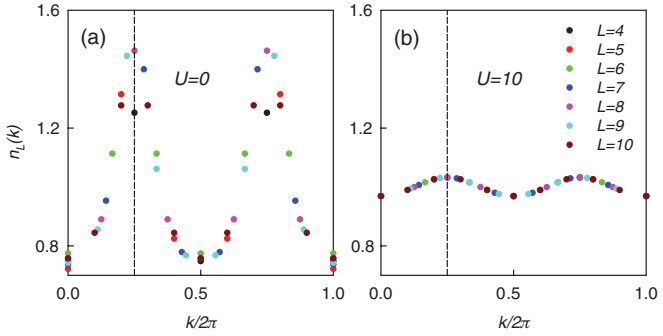

FIG. 2. (Color online) The momentum distributions at (a) $U = 0$ and (b) $U = 10$ on different sizes. The parameters are the same with those in Fig. 1.

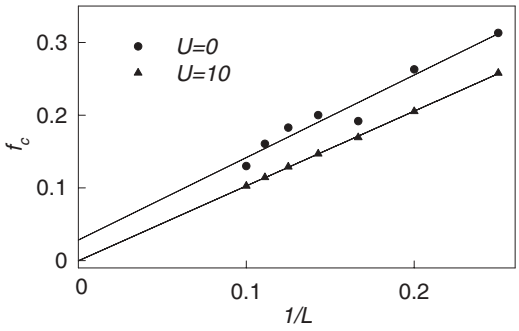

FIG. 3. Finite-size scaling of the condensate fraction f_c at $U = 0$ and $U = 10$. The parameters are the same as those in Fig. 1.

phase at $\nu = 1$. When the Hubbard interaction is turned on, the system is expected to experience a phase transition to the Mott-insulator phase. This is from the result at $U = 10$ [see Fig. 2(b)] where the momentum distribution $n_L(k)$ tends to be uniform and its values nearly don't change with L. To further characterize the phases, we measure the condensate fraction $f_c = (\Lambda_c + \Lambda_d)/N_b$ (N_b is the total number of the hard-core bosons), with Λ_c (Λ_d) being the largest eigenvalue of the one-particle density matrix $\rho_{ij}^c = \langle c_i^\dagger c_j\rangle (\rho_{ij}^d = \langle d_i^\dagger d_j\rangle)$ [36]. Figure 3 shows that at $U = 0$ f_c scales to a nonzero value in the thermodynamic limit while at $U = 10$ it scales to zero. So for small U the system has a nonzero SF density, while for large U the system becomes a Mott insulator. We emphasize that the study of the SF to Mott-insulator transition needs scaling for systems with larger sizes, which is beyond the present method.

The filling factor $\nu = 1/3$. Next we study the case of the filling factor $\nu = 1/3$. We drop the Hubbard interaction, but add NN and NNN interactions to Eq. (1), which gives

$$H_I = V_1\sum_{\langle i,j\rangle} n_i n_j + V_2\sum_{\langle\langle i,j\rangle\rangle} n_i n_j,$$

where $n_i = n_i^c + n_i^d$ is the total number of hard-core bosons on site $\mathbf{r}_i$ and V_1 and V_2 are the strength of the interactions. We have carried out the calculations at $\nu = 1/3$ and found the bosonic FTP where the ground state is threefold degenerate. We first look at the phase diagram in the (V_1, V_2) plane, which is shown is Fig. 4. By turning on V_1, the ground state is threefold degenerate and the bosonic FTP emerges. The ground state is separated from higher eigenstates by a finite gap, whose value increases with the strength of V_1. After turning on V_2, the value of the gap is decreased and vanishes at a critical value V_{2c}, which marks the boundary in the phase diagram. Finite-size scaling shows that the bosonic FTP exists in the thermodynamic limit (see the inset in Fig. 4).

We note that the present phase diagram is very similar to that of the corresponding fermionic system except for the smaller critical values V_{2c} [31]. In Fig. 5(a), it is shown more clearly: at small V_2 the energies E_n of the two lowest states are almost the same in the two systems, while at larger V_2 they are different. The main difference of hard-core bosons and fermions is the exchanging relation. So when the number of the particles is fewer, the exchanging between the particles is less possible and the hard-core bosons are more like spinless fermions. Also at small V_2, there is one particle within each isolated bond, and thus their difference is further weakened.

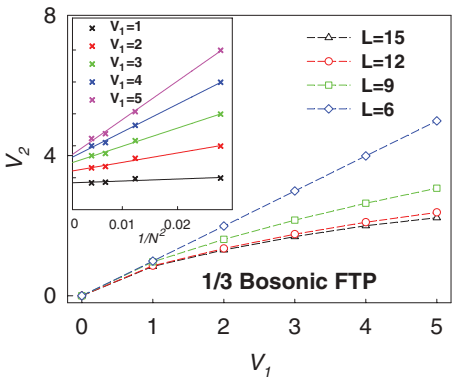

FIG. 4. (Color online) The phase diagram in the (V_1, V_2) plane at $\nu = 1/3$ for different sizes. The inset shows the finite-size scaling of the critical value V_{2c} at different V_1. Here $A = B = 1$ and $M = -2$ when the Hamiltonian Eq. (1) has a nontrivial flatband in the fermionic case.

It is interesting that the situation is similar in two dimensions where the hard-core bosons in the topological band at integer filling don't exhibit the topological phase, while at fractional fillings they do [7,29].

In momentum space, the degenerate ground states are in different momentum sectors and are equally spaced with the interval of N_p, as shown in Fig. 5(b). We also calculate the total Berry phase of the ground states, which is shown in Fig. 5(c). The figure shows that the total Berry phase has a nontrivial value π for small V_2 and begins to be random between $(0,\pi)$ from a critical value V_{2c}, at which the bosonic FTP is broken (here the randomness is due to the fact that the multifold degeneracy of the ground states is greater than three). The obtained critical value V_{2c} is consistent with that from the energy spectra.

Mapping hard-core bosons to spinless fermions. For 1D systems, bosons and fermions can be transformed into each other and there have been examples showing that the topological features can be manifested by Bose to Fermi statistics transmutations in other 1D systems [37]. So in the following we map hard-core bosons to spinless fermions using Matsubara-Matsuda and Jordan-Wigner transformations

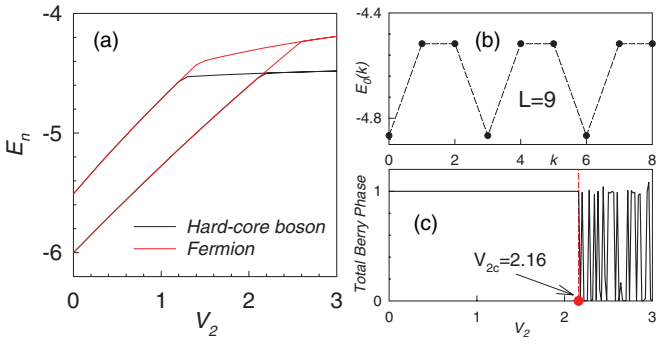

FIG. 5. (Color online) (a) The energies of the ground states and the first-excited states vs V_2 at $V_1 = 3$. (b) The ground-state energy of each momentum sector at $V_1 = 3$ and $V_2 = 1.6$. (c) The total Berry phase vs V_2 at $V_1 = 3$. The parameters are the same as those in Fig. 4 except for $M = -1.999$ in panel (c) when the band slightly departs from the exact flatness. Here the system size is $L = 9$.

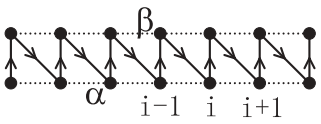

FIG. 6. Zigzag path in the two-leg ladder.

[38–40] to gain some insight into the different behaviors of hard-core bosons at different filling factors from the mapped fermionic model. Using the Matsubara-Matsuda transformation, the Hamiltonian Eq. (1) can be mapped to a spin-1/2 one with the identifications $c_i^\dagger(d_i^\dagger) = S_{ic}^+(S_{id}^+)$, $c_i(d_i) = S_{ic}^-(S_{id}^-)$, and $n_{ic,d} = \frac{1}{2} + S_{ic,d}^z$. The two-component system can be regarded as a two-leg ladder with one component on each site [41,42]. For two-leg ladders the Jordan-Wigner transformation can be applied directly when all sites are arranged in a 1D sequence (the zigzag path in Fig. 6). Then we divide the ladder into two sublattices and introduce two species of spinless fermions α_i and β_i. The spin operators on the two sublattices transform to

$$S_{i\alpha}^+ = \alpha_i^\dagger e^{i\pi \sum_{j<i}(\alpha_j^\dagger\alpha_j + \beta_j^\dagger\beta_j)}, \quad S_{i\beta}^+ = \beta_i^\dagger e^{i\pi \sum_{j<i}(\alpha_j^\dagger\alpha_j + \beta_j^\dagger\beta_j)} e^{i\pi\alpha_i^\dagger\alpha_i}.$$

Using the above transformation, besides the terms in Eq. (1) the following additional terms containing four- and six-fermion operators appear:

$$\Delta H = 2B\sum_i \alpha_i^\dagger\alpha_{i+1}n_{i\beta} - 2B\sum_i \beta_i^\dagger\beta_{i+1}n_{i+1\alpha} + 2iA\sum_i \alpha_i^\dagger\beta_{i+1}(n_{i\beta} + n_{i+1\alpha} - 2n_{i+1\alpha}n_{i\beta}) + \text{H.c.}, \tag{2}$$

with $n_{i\alpha} = \alpha_i^\dagger\alpha_i$ and $n_{i\beta} = \beta_i^\dagger\beta_i$. At low fillings when there is no double occupying and neighboring, these additional terms vanish, so hard-core bosons show the same behaviors with fermions. While at high fillings, these terms show their effect and answer for the absence of the topological properties at $\nu = 1$ in hard-core boson systems.

Conclusions. We have studied the hard-core bosons in 1D interacting topological bands at different filling factors. For the case of $\nu = 1$, we consider the on-site Hubbard interaction. By calculating the energies of the lowest states, the Berry phase, and the fidelity metric of the ground states, we find no sign of the existence of the bosonic topological phase, which is in contrast to the fermionic case. To identify the phase of the ground state, we further study the momentum distribution and the condensate fraction and find a SF to Mott-insulator transition driven by the Hubbard interaction. For the case of $\nu = 1/3$, we add NN and NNN interactions instead. We identify the bosonic FTP whose ground state is characterized by a threefold degeneracy and a quantized total Berry phase. We also find that the obtained phase diagram is very similar to that of the corresponding fermionic system except for the different critical values. Finally we discuss the reason for the different behaviors of hard-core bosons at different filling factors. Though the model we study is artificial, due to the rapid development of the field of cold atoms [43], we are hopeful that the model will be engineered and that the phases it will exhibit will be studied experimentally.

Acknowledgments. The author would like to thank Shiping Feng, Bin Liu, Jihong Qin, and Shun-Qing Shen for helpful discussions. Specially the author thanks the referee for valuable suggestions. Support for this work came from the NSFC under Grants No. 11274032 and No. 11104189 and from the Fok Ying Tung Education Foundation.

[1] C. L. Kane and E. J. Mele, Phys. Rev. Lett. **95**, 226801 (2005).
[2] C. L. Kane and E. J. Mele, Phys. Rev. Lett. **95**, 146802 (2005).
[3] J. E. Moore, Nature (London) **464**, 194 (2010).
[4] M. Z. Hasan and C. L. Kane, Rev. Mod. Phys. **82**, 3045 (2010).
[5] Xiao-Liang Qi and Shou-Cheng Zhang, Rev. Mod. Phys. **83**, 1057 (2011).
[6] S. Raghu, Xiao-Liang Qi, C. Honerkamp, and Shou-Cheng Zhang, Phys. Rev. Lett. **100**, 156401 (2008).
[7] Christopher N. Varney, Kai Sun, Marcos Rigol, and Victor Galitski, Phys. Rev. B **82**, 115125 (2010).
[8] M. Hohenadler, T. C. Lang, and F. F. Assaad, Phys. Rev. Lett. **106**, 100403 (2011).
[9] Shun-Li Yu, X. C. Xie, and Jian-Xin Li, Phys. Rev. Lett. **107**, 010401 (2011).
[10] Dong Zheng, Guang-Ming Zhang, and Congjun Wu, Phys. Rev. B **84**, 205121 (2011).
[11] Youhei Yamaji and Masatoshi Imada, Phys. Rev. B **83**, 205122 (2011).
[12] Dung-Hai Lee, Phys. Rev. Lett. **107**, 166806 (2011).
[13] Zhong Wang, Xiao-Liang Qi, and Shou-Cheng Zhang, Phys. Rev. Lett. **105**, 256803 (2010).
[14] Zhong Wang, Xiao-Liang Qi, and Shou-Cheng Zhang, Phys. Rev. B **85**, 165126 (2012).
[15] Zhong Wang and Shou-Cheng Zhang, Phys. Rev. X **2**, 031008 (2012).
[16] L. Fidkowski and A. Kitaev, Phys. Rev. B **81**, 134509 (2010).
[17] Evelyn Tang and Xiao-Gang Wen, Phys. Rev. Lett. **109**, 096403 (2012).
[18] E. Tang, J. W. Mei, and X. G. Wen, Phys. Rev. Lett. **106**, 236802 (2011).
[19] T. Neupert, L. Santos, C. Chamon, and C. Mudry, Phys. Rev. Lett. **106**, 236804 (2011).
[20] K. Sun, Z. Gu, H. Katsura, and S. Das Sarma, Phys. Rev. Lett. **106**, 236803 (2011).
[21] F. Wang and Y. Ran, Phys. Rev. B **84**, 241103 (2011).
[22] X. Hu, M. Kargarian, and G. A. Fiete, Phys. Rev. B **84**, 155116 (2011).
[23] T. Neupert, L. Santos, S. Ryu, C. Chamon, and C. Mudry, Phys. Rev. B **84**, 165107 (2011).
[24] C. Weeks and M. Franz, Phys. Rev. B **85**, 041104 (2012).
[25] X. L. Qi, Phys. Rev. Lett. **107**, 126803 (2011).
[26] D. N. Sheng, Z. C. Gu, Kai Sun, and L. Sheng, Nat. Commun. **2**, 389 (2011).
[27] N. Regnault and B. A. Bernevig, Phys. Rev. X **1**, 021014 (2011).
[28] Yang-Le Wu, B. A. Bernevig, and N. Regnault, Phys. Rev. B **85**, 075116 (2012).
[29] Y. F. Wang, Z. C. Gu, C. D. Gong, and D. N. Sheng, Phys. Rev. Lett. **107**, 146803 (2011).
[30] Huaiming Guo and Shun-Qing Shen, Phys. Rev. B **84**, 195107 (2011).
[31] Huaiming Guo, Shun-Qing Shen, and Shiping Feng, Phys. Rev. B **86**, 085124 (2012).
[32] Raffaele Resta, Rev. Mod. Phys. **66**, 899 (1994).
[33] Di Xiao, Ming-Che Chang, and Qian Niu, Rev. Mod. Phys. **82**, 1959 (2010).
[34] Q. Niu, D. J. Thouless, and Y.-S. Wu, Phys. Rev. B **31**, 3372 (1985).
[35] Min-Chul Cha, Jong-Geun Shin, and Ji-Woo Lee, Phys. Rev. B **80**, 193104 (2009).
[36] C. N. Varney, Kai Sun, V. Galitski, and M. Rigol, Phys. Rev. Lett. **107**, 077201 (2011).
[37] H. V. Kruis, I. P. McCulloch, Z. Nussinov, and J. Zaanen, Phys. Rev. B **70**, 075109 (2004).
[38] T. Matsubara and H. Matsuda, Prog. Theor. Phys. **16**, 569 (1956).
[39] P. Jordan and E. Wigner, Z. Phys. **47**, 631 (1928).
[40] N. Trivedi and D. M. Ceperley, Phys. Rev. B **41**, 4552 (1990).
[41] X. Dai and Z. B. Su, Phys. Rev. B **57**, 964 (1998).
[42] Tamara S. Nunner and Thilo Kopp, Phys. Rev. B **69**, 104419 (2004).
[43] I. Bloch, J. Dalibard, and W. Zwerger, Rev. Mod. Phys. **80**, 885 (2008).